

The interactive indoor-outdoor building energy modeling for enhancing the predictions of urban microclimates and building energy demands

Liping Wang^{a,*}, Lichen Wu^a, Leslie Keith Norford^b, Amir A. Aliabadi^c, Edwin Lee^d

^a Department of Civil and Architectural Engineering and Construction Management, University of Wyoming, 1000 E University Ave, Laramie, WY, 82071, USA

^b Department of Architecture, Massachusetts Institute of Technology, 77 Massachusetts Avenue, Cambridge, MA, 02139, USA

^c School of Engineering, University of Guelph, 50 Stone Rd E, Guelph, ON, N1G 2W1, Canada

^d Commercial Buildings Research Group, National Renewable Energy Laboratory, Golden, CO, 80401, USA

ARTICLE INFO

Keywords:

Microclimate
Coupling
Building energy model

ABSTRACT

There is a lack of an urban building energy modeling framework that considers the influence of surrounding buildings and local urban climate on building thermal performance. This can lead to inaccurate results since the thermal performance of individual buildings is heavily influenced by their surrounding built and climatic environment. This study establishes an interactive indoor-outdoor building energy modeling method to enhance the predictions of urban microclimates and building energy demands by coupling an urban physics model with a physics-based building energy model. Validation of the interactive coupling scheme uses field measurement datasets. Parametric simulation and analysis are conducted to understand the influence of the roof-to-canyon width ratio, canyon orientation, and ground vegetation fraction on canyon temperature, building energy consumption, and energy demand. Furthermore, the impacts of building energy model complexity (e.g., detailed vs. simplified building models) and coupling approaches on canyon temperature and building energy profiles are demonstrated using two case study buildings. In comparison with the one-way coupling approach, cooling energy consumption predicted with the dynamic two-way coupling approach varies by 3.5 % and 0.5 % for the detailed medium office building model and high-rise building model, respectively, and peak cooling demand varies by 8.4 % and 7.0 % for the detailed medium office building model and high-rise building model, respectively. This study also suggests that adopting a complex two-way coupling approach with environmental data exchange at various elevations is necessary for modeling tall buildings at the urban scale.

1. Introduction

The United States has set a climate target to cut carbon emissions by 52 % from 2005 levels by 2030 [1]. Human activities in urban areas contribute to 75 % of greenhouse gas (GHG) emissions [2]. The United Nations projects that 68 % of the world's population will live in urban areas by 2050 [3]. Urban climate action is crucial for future climate adaptation and mitigation. GHG emissions from human activities already caused the rise of global average surface temperature by 1.1 °C compared to pre-industrial levels [4]. At current emission rates, the average global temperature will rise by 1.5 °C between 2030 and 2052 [5]. Urban heat island (UHI) effects refer to air temperature in a metropolitan area that is warmer than the temperature of surrounding rural areas due to reduced vegetated areas, anthropogenic sources [6], high thermal inertia [7], and reduced wind speed [8]. UHI exacerbates

the impacts of increased surface temperature in cities due to climate change. The increase in global near-surface air temperature results in substantial increases in building energy consumption and peak electricity demands, elevated concentration of harmful pollutants, adverse impacts on low-income populations, and heat-related morbidity and mortality [9].

Urban-scale building energy modeling can be categorized into top-down and bottom-up approaches [10]. A top-down approach begins with building energy demand on a large scale and then divides the building stock into smaller subsections. A bottom-up approach [10] involves modeling building stocks based on first-principle, grey-box, or black-box models. In existing urban-scale energy modeling studies, first-principle-based models included EnergyPlus [11–15], ESP-r [16], and energy-balance equations [17,18]. Thermal network models [19–21] have been used for urban energy modeling as the grey-box

* Corresponding author.

E-mail address: lwang12@uwyo.edu (L. Wang).

<https://doi.org/10.1016/j.buildenv.2023.111059>

Received 11 June 2023; Received in revised form 14 October 2023; Accepted 16 October 2023

Available online 22 November 2023

0360-1323/© 2023 Elsevier Ltd. All rights reserved.

models for buildings and urban canopy models. Statistical regressions [22] and neural network models [23] have been used as black-box models for modeling building energy use at urban scales. The bottom-up approach has been commonly used for urban-scale building energy modeling.

Most urban scale modeling studies [15,18,20–22,24–27] have simulated energy profiles of building stocks at the city level using archetypes [28] and sample buildings [29] but few studies have considered the influence of urban microclimates and urban geometrical settings. This can lead to inaccurate results since the thermal performance of individual buildings is heavily influenced by their surrounding built and climatic environment. Hong et al. [30] evaluated microclimate's impact on building stocks in San Francisco by simulating annual energy use and peak demands of large office buildings and hotels using 10-year measured hourly weather data for 27 sites in the city. Although direct measurement of long-term weather data can accurately reflect urban heat islands, the synthesized weather files for building energy simulation heavily rely on the availability and quality of data.

Besides direct microclimate measurements across different locations in a city, urban canopy models and computational fluid dynamics (CFD) are alternative methods to predict the microclimatic environment in urban settings. Urban canopy models have been implemented into regional climate models such as the Weather Research and Forecasting (WRF) model [31] and urban physics models such as urban weather generator (UWG) [32] or vertical city weather generator (VCWG) [33, 34], which account for urban physics (building morphology, materials and internal energy use) to estimate changes in weather variables and estimate UHI effects.

WRF as a regional climate model has been integrated with a single-layer urban canopy model (SLUCM) and multi-layer urban canopy model (Building Environment Parametrization (BEP)) [35] for urban modeling. Various studies [36–38] have employed WRF and urban canopy models for simulating UHI effects. A simplified building energy model (BEM) has been integrated with WRF and BEP [14] although certain limitations of BEP-BEM have been identified [39]. BEP provides outdoor air temperature, relative humidity, and radiation for BEM; BEM feeds wall and roof temperature and heat flux from heating, ventilation, and air conditioning (HVAC) systems to BEP [14]. Ribeiro et al. [39] tested the integrated modeling schemes between WRF, BEP, and BEM. Wong et al. [13] created an integrated multiscale urban model coupling WRF, a single layer urban canopy model, a CFD model with OpenFOAM, and EnergyPlus for modeling the National University of Singapore's Kent Ridge campus to demonstrate multi-domain simulations from mesoscale to microscale for urban energy modeling.

Urban physics models such as UWG [32] and VCWG [33] predict local urban microclimatic conditions, including dry bulb temperature and relative humidity, by accounting for UHI effects on data from a weather station located outside the city. UWG is composed of four coupled submodels: a rural station model, a vertical diffusion model, an urban boundary-layer model, and a coupled urban canopy and building energy model. The rural station model calculates sensible heat fluxes at the weather station; the vertical diffusion model calculates vertical profiles of air temperature above the rural site; the urban boundary-layer model calculates air temperatures above the urban canopy layer (above urban canyons); and the integrated urban canopy and building energy model calculates urban sensible heat fluxes and urban canyon air temperature and humidity. Reinhart et al. [12] developed umi—a Rhinoceros-based urban modeling tool for energy use, daylighting, and walkability evaluations based on EnergyPlus, Radiance/Daysim, Grasshopper, and Python scripts. Umi utilizes the local climate weather file generated from UWG. VCWG v2.0.0 [33] builds on UWG [32] and includes a hydrology model to account for the biophysical and ecophysiological behavior of urban vegetation as well as a vertical diffusion model for momentum, heat, humidity, and turbulence kinetic energy. In addition, there are two options for microclimate prediction in VCWG: (1) rural forcing near the surface; and (2) top

forcing above the urban domain using such reanalysis datasets as ERA-5 data from European Centre for Medium-Range Weather Forecasts (ECMWF).

For such programs as UWG and VCWG, urban canopy models have been integrated with simplified building energy models to predict microclimates in urban environments with the consideration of anthropogenic heat from building heating and cooling. However, the simplified building energy models treat buildings as a single well-mixed thermal zone and predict energy consumption based on simplified equations for HVAC equipment. The simplified building energy models cannot accurately predict waste heat from commercial buildings [40], especially high-rise buildings, due to their simplifications in thermal envelope load calculations and HVAC systems and lack the capability of modeling detailed building systems as well as novel building technologies (e.g. renewable energy and energy storage).

Based on our literature review, we identified the research gap—a lack of an urban building energy modeling framework that considers the influence of the surrounding built and climatic environment on building thermal performance. This can lead to inaccurate urban scale energy modeling results since the thermal performance of individual buildings is heavily influenced by their surrounding built and climatic environment. Although urban physics models predict microclimates in urban environments with the consideration of anthropogenic heat from building heating and cooling, these programs treat buildings as a single well-mixed thermal zone, which cannot accurately predict building waste heat, especially for high-rise buildings.

The objective of this study is to establish an interactive indoor-outdoor building energy modeling framework to enhance the predictions of urban microclimates and building energy demands by dynamically coupling an urban physics model with physics-based building energy model. In the study, we evaluated the impacts of different coupling schemes between the urban physics model and the physics-based building energy model on microclimate predictions and building energy use. The established coupling schemes from this study can be adopted for urban-scale building energy modeling to enhance the predictions of urban microclimate variables and large-scale building energy demands.

Particularly, VCWG v2.0.0 is used to predict urban microclimate conditions and is dynamically coupled with the EnergyPlus v22.1 building energy model through the Python application programming interface (API). Validations for the dynamic coupling between the urban canopy model and EnergyPlus are conducted using measurements from projects in Basel, Switzerland [41], Toulouse, France [42], and Vancouver, Canada [43]. Parametric simulation and analysis were conducted to understand the influence of urban geometric and surface features on canyon temperature and building energy profiles. Different levels of building energy model complexity as well as different coupling approaches were compared to evaluate their impacts on canyon temperature and building energy profiles using two case study buildings. This paper summarizes the advantages and disadvantages of adopting different coupling strategies for urban microclimate and building energy predictions.

2. Methodology

The interactive coupling scheme between the urban physics model VCWG and the building energy simulation program EnergyPlus, achieved through a Python API, is shown in Fig. 1. In each timestep of the coupled simulation, VCWG provides predicted local climate conditions, such as canyon temperature, relative humidity (RH) and roof convective heat transfer coefficient, to EnergyPlus as boundary conditions; EnergyPlus calculates waste heat generated from building HVAC systems and building exterior surface temperatures and passes both to VCWG. The simplified building energy model and exterior surface temperature calculation from VCWG are replaced by the results produced by EnergyPlus [44].

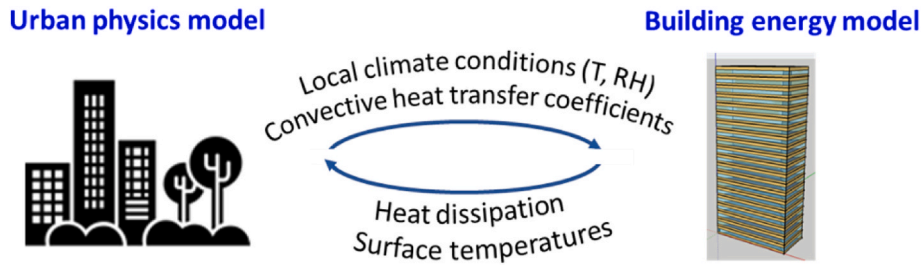


Fig. 1. Interactive coupling method between urban physics model and building energy model for building energy modeling in urban environments.

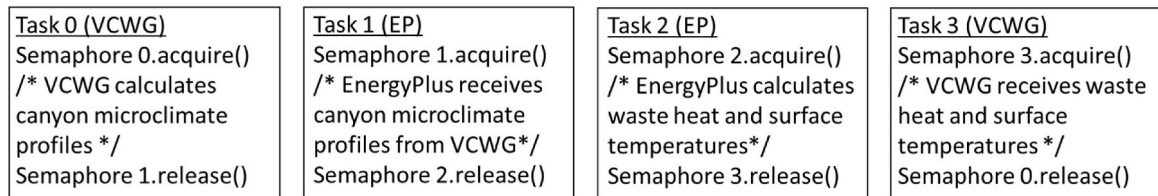
Semaphore objects in threading from Python Threading Library were used to synchronize and coordinate EnergyPlus and VCWG runs for data exchange during each timestep. The rationale of using semaphores is for synchronization among multiple tasks and access control in the concurrent multitasking environment. VCWG interacts with individual EnergyPlus threads, which pass control in and out in a synchronized fashion to connect other simulation programs. The semaphore objects define which program to run and when to run. Each semaphore object was first initialized with an unsigned integer value. The initial value of the semaphores is the desired number of initial allowed concurrent accesses. An initial value of one for semaphores represents a mutual exclusion lock and only one thread at a time can be executed. The semaphore object with an initial value of one enters the task section without waiting. The other semaphore objects with assigned initial values of zero must wait. Each semaphore object is accessed through two operations: acquire() and release(). Acquire() requests a permit to run and decrement the integer value (minimum 0) of the available permit by each call, and release() calls release a permit and increment the integer value of the available permit. Therefore, between acquire() and release() operations, each semaphore uses the permit to run a specific task. The calling points of acquire() and release() are critical to ensure that multiple tasks are executed in a requested sequence.

There are four sequential tasks (Tasks 0–3) during each timestep. We

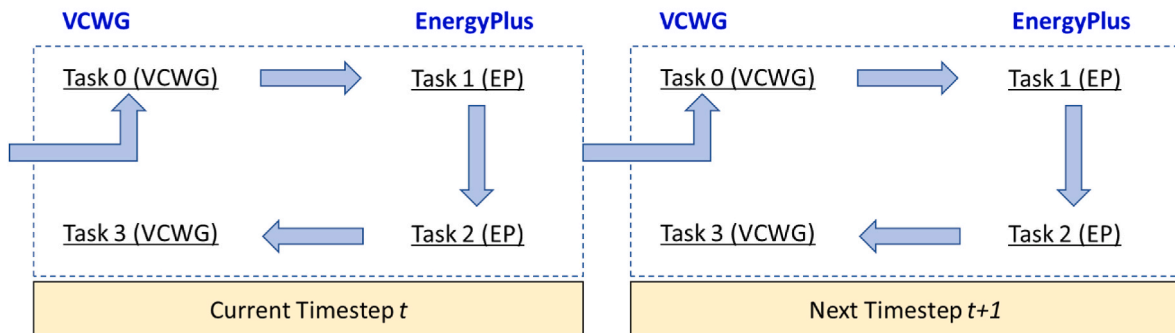
use four semaphore objects (Semaphores 0–3) to define the sequence of running each task between EnergyPlus and VCWG as shown in Fig. 2. Starting from the beginning, in each time step, Semaphore 0 obtains a permit to request VCWG to calculate canyon microclimate profiles such as temperature and humidity (Task 0). After the completion of the calculation from VCWG, Semaphore 1 obtains the permit and the canyon microclimate conditions including outdoor dry bulb temperature, outdoor relative humidity, and roof convective heat transfer coefficient calculated by VCWG are used to override outdoor conditions in EnergyPlus for the same time step (Task 1). After that, Semaphore 2 requests EnergyPlus to calculate waste heat generated from building systems and building surface temperatures (Task 2). Finally, Semaphore 3 obtains the permit and allows VCWG to receive the waste heat and surface temperatures from EnergyPlus for the time step (Task 3). The interactive coupling then moves to the next time step.

3. Validation of the interactive coupling approach

We validated the interactive coupling scheme with data from three field measurements campaigns: the Basel UrBan Boundary Layer Experiment (BUBBLE) in Basel, Switzerland [41]; the CAPITOU experiment in Toulouse, France [42]; and the Sunset neighborhood field measurement in Vancouver, Canada [43]. We used both VCWG and the



(a)



(b)

Fig. 2. Python semaphore schema for interactive coupling method between VCWG and EnergyPlus (a) semaphore definition (b) sequence definition.

coupled EnergyPlus and VCWG for microclimate data predictions first and then compare the predicted canyon temperatures at specified heights to the measurements from the three field measurements. In addition, we compared building surface temperatures and HVAC waste heat generation rates between VCWG and the coupled simulation between EnergyPlus and VCWG.

3.1. BUBBLE in basel, Switzerland

In the BUBBLE project, experiments were conducted in the city of Basel, Switzerland [41]. A measurement tower at the site (Ue1) extended from street level up to 30 m [41]. Temperature and wind profiles at specific vertical heights were measured from fall 2001 to summer 2022. In addition, measurement of heat fluxes contributed to/from the canyon, satellite ground truth for long-wave radiations, and urban turbulence and profiling were taken during an intensive observation period of June 10, 2002–July 12, 2002.

In this study, we compared air temperatures at 10-min intervals among measurements from BUBBLE, rural weather data, microclimate predictions from VCWG 2.0.0 and the interactive coupling. We modified the DOE EnergyPlus reference building model for a middle-rise apartment based on the building envelope and system properties [32,33,41]. The building height for Ue1 is 14.6 m. Urban albedo is 0.15 and urban emissivity is 0.95. The canyon width is 18.2 m and the canyon axis orientations are 65°.

Fig. 3 shows the 10-min time series comparison between measurements and predictions from VCWG 2.0.0 as well as the interactive coupling between VCWG and EnergyPlus (VCWG_EP) for Ue1 at the height of 13.9 m. We calculated the statistical results of air temperature predictions from VCWG and VCWG_EP in comparison with measurements for six canyon heights (2.6 m, 13.9 m, 17.5 m, 21.5 m, 25.5 m and 31.2 m). We used the coefficient of variation of root mean square error (CV-RMSE) and normalized mean bias error (MBE) from ASHRAE Guideline 14 [45] to compare measurement and simulation results from VCWG and VCWG_EP. Eqs. (1) and (2) are used for calculating CV-RMSE and MBE.

$$CV - RMSE = \frac{1}{\bar{Y}} \sqrt{\frac{\sum_{i=1}^n (Y_i - \hat{Y}_i)^2}{N}} \quad (1)$$

$$MBE = \frac{\sum_{i=1}^n (Y_i - \hat{Y}_i)}{N \times \bar{Y}} \quad (2)$$

where N is the number of samples, Y represents the measurements, and \hat{Y} represents the predictions from VCWG or VCWG_EP.

We found that the air temperature predictions from both VCWG and VCWG_EP are comparable and very close. This also indicates the interactive coupling scheme was correctly implemented in VCWG_EP. CV-RMSE ranges from 7.38 % to 10.70 % for VCWG and from 7.46 % to 10.71 % for VCWG_EP. MBE ranges from 0.29 % to 1.44 % for VCWG and from 0.60 % to 1.65 % for VCWG_EP. The deviations between measurements and predictions can be attributed to the simplification of urban canyon settings in microclimate modeling, non-uniform temperature distribution within urban canyons, and uncertainties of air temperature measurements.

3.2. CAPITOUL in Toulouse, France

The Toulouse urban layer (CAPITOUL) experiment aimed to quantify the interactions between the urban surface, urban canopy layer, and urban aerosols. The joint experimental effort of the CAPITOUL project in Toulouse, France was conducted from March 2004 to February 2005. The downtown area of Toulouse has a relatively homogeneous building height of ~20 m and construction materials with brick walls and tile roofs. Sensors for temperatures and radiative fluxes were mounted on a 27.5 m pneumatic tower installed on a roof at a height of 20 m. Six resistance thermometers in gill-ventilated shields were installed along the mast at different heights. Adjacent to the mast site, turbulence sensors and optical particle counters were mounted on booms, extending across approximately one-third of the width of the street away from the canyon wall. In addition, mini-stations continuously measured the temperature and humidity of 21 sites in various districts of the urban area. Besides temperature, humidity, and aerosol data, seasonal anthropogenic fluxes, net all-wave radiation, and the turbulent sensible and latent heat fluxes between surface and atmosphere were also

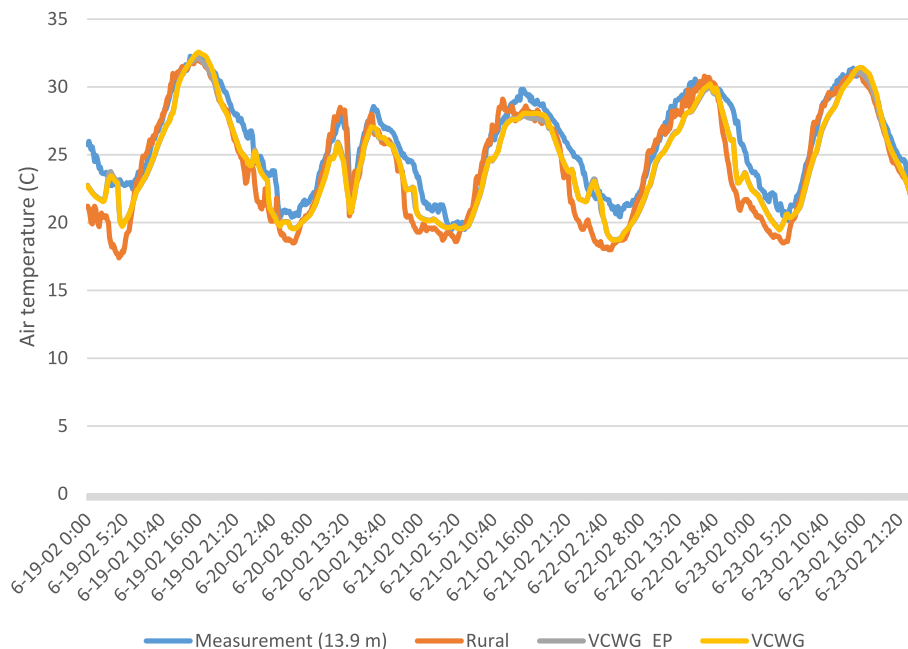


Fig. 3. Ten-minute time series comparison for BUBBLE Ue1 site between measurements and predictions from VCWG and VCWG_EP between June 19, 2002 and June 23, 2002. (VCWG_EP: the interactive coupling between VCWG and EnergyPlus).

reported from March 2004 to February 2005 for the city center of Toulouse [42].

We used the DOE reference building prototype for a medium office building for the CAPITOU project validation. We created a rural weather data file based on the measurements of air temperature, relative humidity, and solar radiation from Mondouzil, France. The urban weather station on Pomme Street next to the Monoprix building represents the urban microclimate of the city center. The urban albedo is 0.25 and urban emissivity is 0.95. The canyon width is 9 m. The canyon axis orientations are -50° .

We calculated CV-RMSE and MBE of canyon temperature between measurements of CAPITOU and predictions from VCWG only and VCWG_EP. CV-RMSEs are 5.02 % and 5.13 % between June 1–30, 2004 for VCWG and VCWG_EP, respectively. Fig. 4 shows the comparison of 5-min time series data among measurement, VCWG_EP, and VCWG at the height of 19 m as well as rural ambient temperature. The predictions from VCWG_EP and VCWG match measurements closely.

3.3. Sunset neighborhood in Vancouver, Canada

A 30-m micrometeorological tower located in the Sunset neighborhood of Vancouver, BC, Canada measured urban climate variables, including air temperature and wind profiles and energy fluxes. For a 500-m radius around the tower, the mean building height was 6.5 m; building types include residential houses for the majority of buildings, commercial offices, retail buildings, and schools. Measurements from May 2008 to September 2008 were used for validation. The urban canyon axis has a north orientation. Approximately 90 % of buildings in the Sunset neighborhood have natural-gas space heating [43].

We used a modified DOE reference building prototype for the small office in the interactive coupling. In particular, we modified the internal heat gains of the small office building model based on those in the residential building type to reflect the major building type of the measurement site. For this project, ERA-5 data from ECMWF were used in the top forcing validation. Urban emissivity is 0.95 and urban albedos for roof, ground, walls, and vegetation are 0.13, 0.14, 0.2, and 0.27, respectively ECMWF [33]. We compared predictions from VCWG and VCWG_EP to air temperature measurements at 1.2 m.

We calculated the CV-RMSE and MBE of canyon temperatures

between measurements and predictions from VCWG only and VCWG_EP in Vancouver, CA between July 1 and July 31, 2008. CV-RMSEs are 9.61 % and 9.76 % between July 1 and July 31, 2008 for VCWG and VCWG_EP, respectively. Fig. 4 shows the comparison of 30-min time series data among measurement, VCWG_EP, and VCWG at the height of 1.2 m as well as rural ambient temperature. In comparison with CAPITOU and BUBBLE, the predictions from VCWG_EP and VCWG show larger deviations from measurements in Vancouver, CA. Especially, peaks of canyon temperature measurements were not well captured.

4. Sensitivity analysis

Using the coupled modeling approach VCWG_EP, we conduct parametric simulations and analysis to evaluate the impacts of urban geometric and surface features on canyon temperature, building energy consumption, and demand. These features include the ratio of roof width to canyon width (0.75, 1, 1.5, 3), which represents canyon density; canyon orientation (-45° , 90°); and ground vegetation fraction (0, 0.5, 1). We implemented these features by modifying the input files for VCWG and EnergyPlus and programmed a Python script to automatically run the parametric simulations. Twenty-four simulations were conducted using the modeling methods of VCWG_EP. The simulation results of averaged canyon temperature and building energy consumption were compared to the baseline scenario with roof to canyon width ratio = 1, canyon orientation = 90° (building orientation = 0° , north), and ground vegetation fraction = 0. The VCWG and EnergyPlus exchange data at 5-min time intervals. We chose to use the medium office building prototype model in Chicago, IL and conducted the simulation for the period of June 1 to June 30 using the typical meteorological year version 3 (TMY3) weather file for Chicago. The sensitivity analysis demonstrates the capability of coupled modeling between VCWG and EnergyPlus to provide guidelines in urban design. Different climates, simulation periods, and building types can result in different results.

Figs. 5 and 6 show the variations of average and maximum canyon temperature with urban geometric and surface features. Across the 24 simulation scenarios, the maximum canyon temperatures within the month of June vary between 33.5°C to 39.0°C and the average canyon temperature varies between 21.4°C and 22.9°C . The maximum canyon temperature of 39.0°C occurs near noon for the scenario with canyon

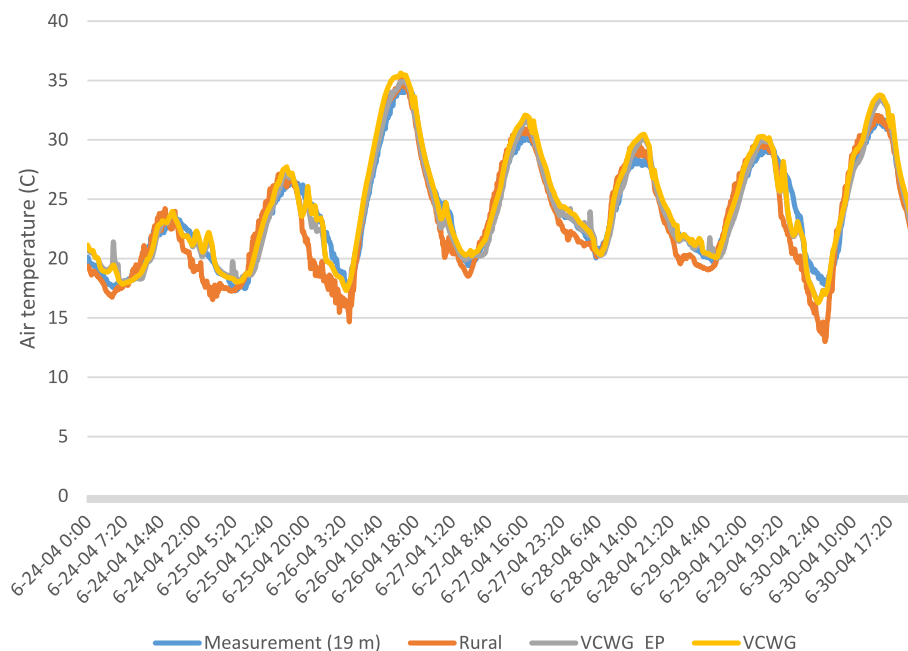


Fig. 4. Five-minute time series comparison for CAPITOU between measurements and predictions from VCWG and VCWG_EP (VCWG_EP: the interactive coupling between VCWG and EnergyPlus).

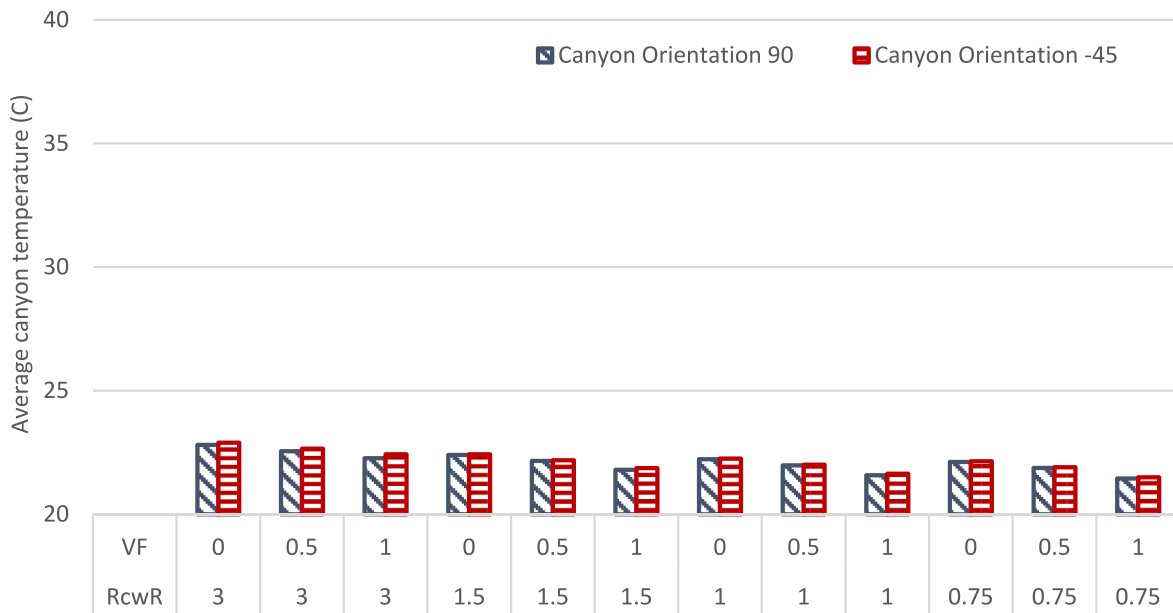


Fig. 5. The variation of average canyon temperatures with urban features (VF: ground vegetation fraction; RcwR: roof to canyon width ratio).

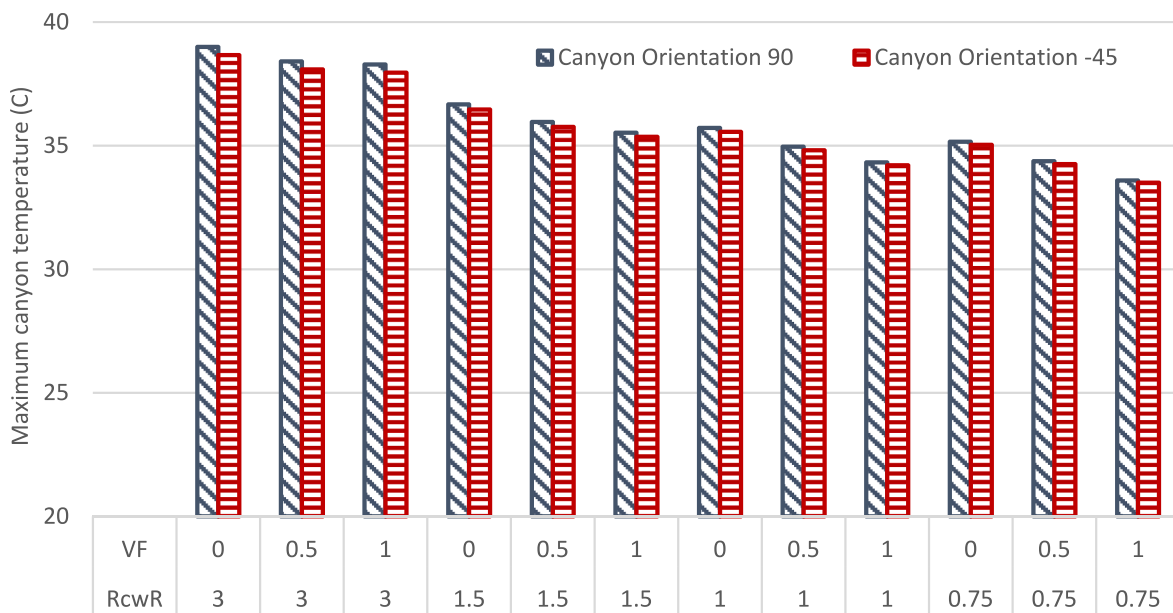


Fig. 6. The variation of maximum canyon temperatures with urban features (VF: ground vegetation fraction; RcwR: roof to canyon width ratio).

orientation = 90°, ground vegetation fraction = 0, and roof to canyon width ratio = 3, while the maximum average canyon temperature of 22.9 °C occurs for the scenario with canyon orientation = 45°, ground vegetation fraction = 0, and roof to canyon width ratio = 3. Although the total heat rejection from buildings with canyon orientation = 45° can be higher than those with canyon orientation = 90°, the wall surface temperatures at noon for scenarios with canyon orientation = 45° are less than those at noon for scenarios with canyon orientation = 90° due to the differences of projected solar radiation fluxes on walls. This results in slightly higher maximum canyon temperatures for scenarios with canyon orientation = 90° than those with canyon orientation = 45°. Based on the modeling results, we can also conclude that the increase in ground vegetation and decrease in building planar area density can effectively reduce urban canyon temperature.

We also evaluate the variations of predicted cooling electricity consumption and peak cooling demands in comparison with those from the

defined baseline scenario for the simulation period among the 24 simulation scenarios. In this study, cooling demand represents the peak cooling demand for the simulation period. Fig. 7 compares the cooling electricity of individual scenarios with the baseline results. It is found that cooling electricity consumption varies between -6.6 % and 14.9 %. Roof to canyon width ratio is the most influential factor among the three urban features. By increasing the roof to canyon width ratio from one to three (increasing urban canyon density), cooling electricity consumption increases by 10.6 % and 9.6 % for canyon orientation -45° and 90°, respectively. Changing building orientation from 0° to 45° increases building cooling electricity consumption by 4.2 %–6.0 %. Increasing the ground vegetation fraction from zero to one can reduce building cooling electricity consumption by 4.1 %–5.2 %. The cooling demand variation as shown in Fig. 8 ranges from -8.8 % to 17.5 %. The variations of cooling demands are largely driven by the maximum local outdoor air temperature. The maximum increase in cooling demands occurs for the

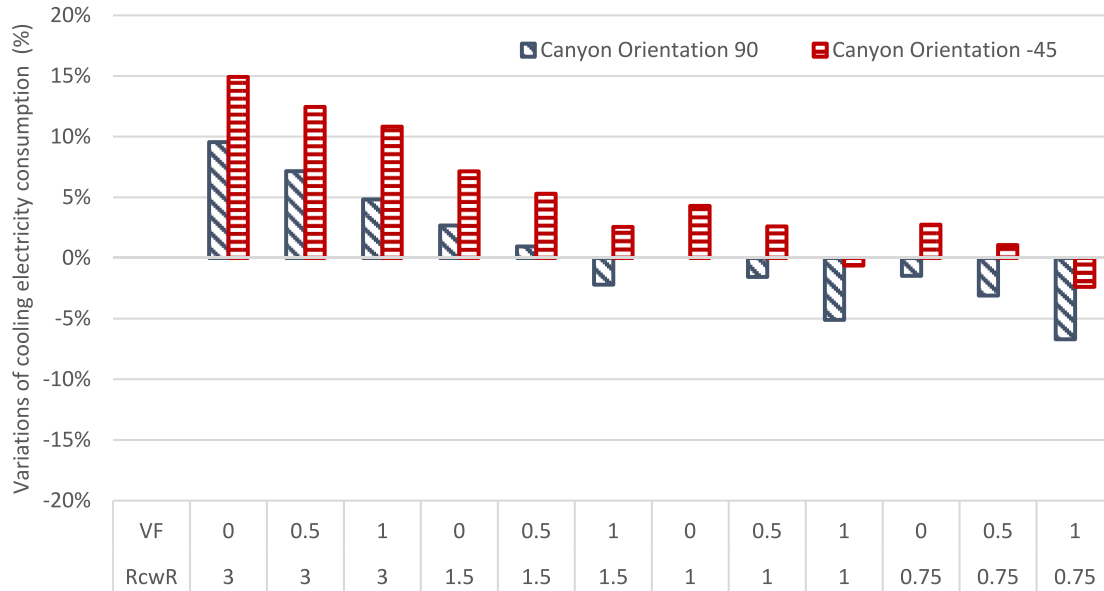


Fig. 7. The variations of cooling electricity consumption in comparison with the baseline scenario related to urban features (VF: ground vegetation fraction; RcwR: roof to canyon width ratio).

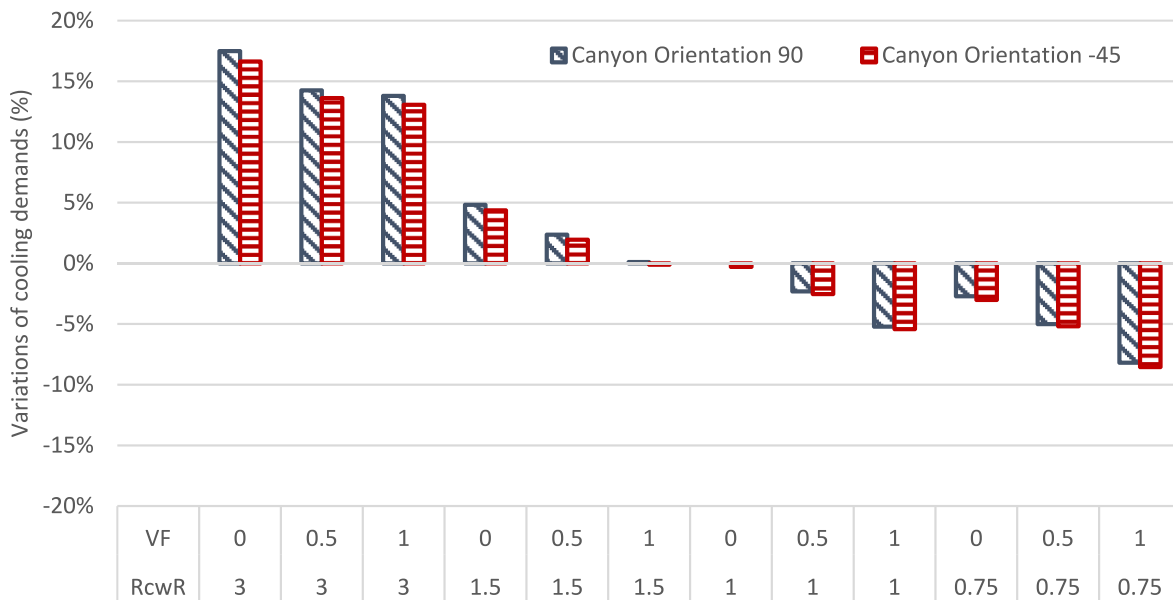


Fig. 8. The variation of cooling demands in comparison with the baseline scenario related to urban features (VF: ground vegetation fraction; RcwR: roof to canyon width ratio).

scenario with canyon orientation = 90°, ground vegetation fraction = 0, and roof to canyon width ratio = 3.

5. Case study

In this section, we conducted case studies using two synthetic buildings—a medium office building and a high-rise office building—to evaluate the impacts of different modeling approaches and whole building model complexity on canyon temperature and building energy use. We compared different levels of building energy model complexity (e.g., detailed vs. simplified building models) as well as different coupling approaches. Urban configurations for the case studies were set as follows: roof to canyon width ratio = 1; canyon orientation = 90;

vegetated ground fraction = 0.

These coupling approaches include embedding a single zone energy model in an urban canopy model (VCWG); running an urban physics model first to generate an urban weather file followed by running building energy models (VCWG_EP, one-way coupling); and interactive coupling between VCWG and EnergyPlus during each time step (VCWG_EP, two-way coupling). In VCWG_EP (one-way coupling), VCWG was run first to generate a local weather file representing urban microclimate conditions and then EnergyPlus models were simulated using the local weather file. A more complex coupling approach (VCWG_EP_Profile, two-way coupling) was evaluated for the high-rise office building case. In VCWG_EP_Profile (two-way coupling), detailed profiles varying with heights for wall surface temperatures and HVAC

heat dissipations were passed from EnergyPlus to VCWG at each time step and similarly, detailed profiles of canyon temperature and relative humidity varying with height besides roof convective heat transfer coefficient were fed to EnergyPlus from VCWG. The impacts of coupling approaches and model complexity on canyon temperature and building energy profiles are evaluated using two case study buildings.

5.1. Baseline model development

The two synthetic buildings are the medium office (Fig. 9) and the high-rise office building (Fig. 10). The detailed model for the medium office building (Fig. 9) has 15 thermal zones with five thermal zones per floor while the simplified model for the medium office is a single-zone model. We look into the single-zone model because building energy consumption and waste heat dissipation were predicted using single-zone models in VCWG and UWG. Both the detailed model and the single-zone model have the same building height and internal heat gains from people, lighting, and miscellaneous loads. The cooling and heating of the medium office building were supplied by variable air volume systems. The detailed energy model for the 20-story office building (Fig. 10) has 100 thermal zones. The simplified energy model for the 20-story office building contains 15 thermal zones for the ground floor, middle floor, and top floor; the thermal zones of the middle floor have a multiplier of 18 to represent 18 typical floors in total. The cooling and heating of individual thermal zones in the large office building were supplied by package terminal heat pumps. All the models were simulated for the period June 1–30 using the typical meteorological year version 3 (TMY3) weather data for Chicago, IL.

Table 1 summarizes cooling energy consumption and cooling demands normalized by building footprint for the medium and high-rise office building models. Because waste heat dissipation normalized by building footprint predicted by EnergyPlus was passed to VCWG for microclimate predictions, building cooling energy consumption and cooling demands are normalized by building footprint in this study. For the high-rise office building, the deviations between the simplified model and the detailed model are within 1 % for cooling energy consumption and cooling demands. However, for the medium office building model, the deviations between the detailed model and the single-zone model are 18.3 % and 27.1 % for cooling consumption and cooling demands, respectively. This is mainly due to the fact that complex multi-zone buildings cannot be well represented by single-zone models.

5.2. Canyon temperature comparison

5.2.1. The impact of energy model complexity on canyon temperature

Canyon temperature predictions for the month of June from different coupling approaches and different model complexities, including average, maximum, and minimum temperatures, were compared and summarized in Tables 2 and 3 for the medium office building and the high-rise office building, respectively. The deviations of canyon temperature predictions are 0.04 °C, 0.30 °C, and 0.01 °C for average, maximum, and minimum temperatures with the medium office building

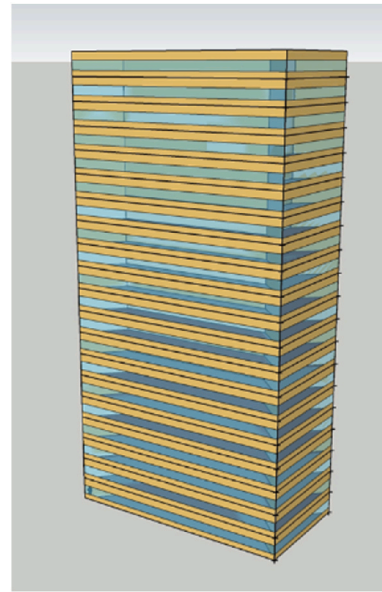


Fig. 10. Detailed high-rise office building model.

Table 1

Comparison of energy profiles from EnergyPlus models for the medium office building (simulation period: June 1– June 30).

Building type	EnergyPlus model type	Normalized cooling consumption based on footprint (MJ/m ²)	Normalized cooling demand based on footprint (W/m ²)
Medium office building	Detailed model	30.4	50.6
	Single-zone model	24.8	36.9
High-rise office building	Detailed model	278.5	379.5
	Simplified model	279.9	381.5

(obtained based on the temperature differences between the “Detailed” model and the “Single zone” model of Table 2); the deviations of canyon temperature predictions are within 0.05 °C, 0.04 °C, and 0.03 °C for average, maximum, and minimum temperatures with the high-rise office building, (obtained based on the temperature differences between the “Detailed” model and the “Simplified” model of Table 3). In comparison with rural temperature data, the average, maximum, and minimum canyon temperatures from two-way coupling and detailed medium building office model are 1.11 °C, 2.41 °C, and 3.76 °C above the rural temperatures respectively. In summary, the level of EnergyPlus model complexity has a limited impact on urban canyon temperature.

5.2.2. The impact of coupling approaches on canyon temperature

For the medium office building (Table 2), the impacts of coupling approaches (VCWG_EP with one-way coupling and two-way coupling) on canyon temperature prediction are small. The differences in average temperature are within 0.46 °C (obtained based on the temperature differences between VCWG_EP one-way coupling and VCWG_EP two-way coupling in the row “Average temperature” of Table 2); the differences in maximum temperature are within 0.38 °C (the row “Maximum temperature” of Table 2); the differences in minimum temperature are within 0.45 °C (the row “Minimum temperature” of Table 2). For the high-rise office building (Table 3), the differences in average temperature between VCWG_EP one-way coupling and VCWG_EP two-way coupling are within 0.10 °C (obtained based on the temperature differences between VCWG_EP one-way coupling and

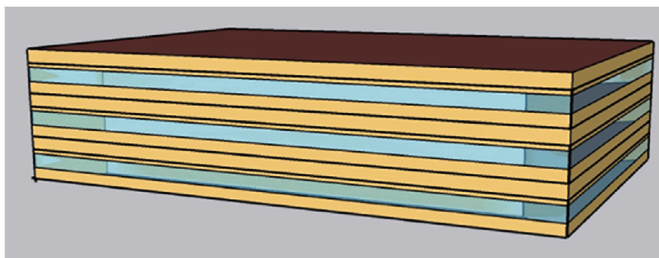


Fig. 9. Detailed medium office building model.

Table 2
Comparison of canyon temperature for different coupling approaches (medium office building).

	Detailed		Single zone		Rural
	VCWG_EP (one-way coupling)	VCWG_EP (two-way coupling)	VCWG_EP (one-way coupling)	VCWG_EP (two-way coupling)	
Average temperature (°C)	22.64	22.22	22.64	22.18	21.11
Maximum temperature (°C)	35.33	35.71	35.33	35.41	33.3
Minimum temperature (°C)	10.91	10.46	10.91	10.47	6.70

Table 3
Comparison of canyon temperature for different coupling approaches (high-rise office building).

	Detailed			Simplified		
	VCWG_EP (one-way coupling)	VCWG_EP (two-way coupling)	VCWG_EP_Profile (two-way coupling)	VCWG_EP (one-way coupling)	VCWG_EP (two-way coupling)	VCWG_EP_Profile (two-way coupling)
Average temperature (°C)	23.62	23.52	25.00	23.62	23.57	24.95
Maximum temperature (°C)	35.35	36.86	41.15	35.35	36.9	41.12
Minimum temperature (°C)	11.85	11.43	11.51	11.85	11.45	11.48

VCWG_EP two-way coupling in the row “Average temperature” of Table 3); the differences in maximum temperature are within 1.55 °C (the row “Maximum temperature” of Table 3); the differences in minimum temperature are within 0.42 °C (the row “Minimum temperature” of Table 3). However, the canyon temperatures predicted with VCWG_EP_Profile (two-way coupling) are much higher than those with VCWG_EP (one-way coupling) and VCWG_EP (two-way coupling). The average and maximum canyon temperatures for the detailed high-rise building model using VCWG_EP_Profile (two-way coupling) approach are 1.38 °C and 5.80 °C higher than those using VCWG_EP (one-way coupling), respectively. The canyon temperatures predicted using the VCWG_EP_Profile approach are vertically averaged along the height of the building. Waste heat is distributed at each floor level for VCWG_EP_Profile while total waste heat is released at the roof level for VCWG_EP and VCWG. Turbulence above building height can easily mix with the waste heat source at roof level resulting in a lower canyon temperature for VCWG_EP and VCWG than the vertically averaged canyon temperature for VCWG_EP_Profile, where waste heat source released at each floor level can be trapped within the canyon due to relatively low turbulent diffusion.

5.3. Cooling energy profiles

5.3.1. The impact of energy model complexity on cooling energy

We evaluate how EnergyPlus model complexity impacts cooling energy consumption and cooling demands for the medium office building and high-rise office building. Based on the simulation results summarized in Table 4, the deviations between the detailed medium office building model and the single zone model using VCWG_EP one-way coupling approach are 16.4 % and 18.1 % for cooling energy consumption and cooling demand, respectively; the deviations between the detailed medium office building model and the single zone model using the VCWG_EP two-way coupling approach are 18.8 % and 25.7 % for

Table 4
Comparison of cooling energy consumption and demands for different coupling approaches (medium office building).

	Detailed		Single zone	
	Normalized cooling consumption based on footprint (MJ/m ²)	Normalized cooling demand based on footprint (W/m ²)	Normalized cooling consumption based on footprint (MJ/m ²)	Normalized cooling demand based on footprint (W/m ²)
VCWG_EP (one-way coupling)	32.67	48.74	27.31	39.91
VCWG_EP (two-way coupling)	31.54	52.85	25.94	39.25

cooling energy consumption and cooling demands, respectively. Our study considers the single-zone building energy model because single-zone models have been used to predict building waste heat dissipation in both VCWG and UWG. These deviations in cooling energy consumption and demands are mainly a consequence of the deviations from EnergyPlus baseline models.

The simulation results for the high-rise office building models are summarized in Table 5. The deviations between the detailed high-rise building model and the simplified model using VCWG_EP one-way and VCWG_EP two-way coupling are within 1.0 %; the deviations between the detailed high-rise building model and the simplified model using VCWG_EP_Profile two-way coupling approach are 2.2 % and 3.8 % for cooling energy consumption and cooling demands, respectively.

5.3.2. The impact of coupling approaches on cooling energy

We compared cooling energy consumption and cooling demands from different coupling approaches for the medium office building and the high-rise office building. Fig. 11 shows the percentage variations in cooling demands and cooling consumption between VCWG_EP two-way and one-way coupling for the medium office building model. For the detailed medium office building model, cooling energy consumption and cooling demands using the VCWG_EP two-way coupling decreased by 3.5 % and increased by 8.4 %, respectively in comparison with the predicted results using VCWG_EP one-way coupling approach. For the single-zone medium office building model, cooling energy consumption and cooling demands using the VCWG_EP two-way coupling approach decreased by 5.0 % and 1.7 %, respectively, in comparison with the prediction results using VCWG_EP one-way coupling approach. Depending on the actual modeling requirements, the improvement in cooling energy consumption and demands prediction for the medium office building case by taking VCWG_EP two-way coupling approach may be compromised by a substantial increase in computing time.

Fig. 12 shows the percentage variations in cooling demands and

Table 5
Comparison of cooling energy consumption and demands for different coupling approaches (high-rise office building).

	Detailed		Simplified	
	Normalized cooling consumption based on footprint (MJ/m ²)	Normalized cooling demand based on footprint (W/m ²)	Normalized cooling consumption based on footprint (MJ/m ²)	Normalized cooling demand based on footprint (W/m ²)
VCWG_EP (one-way coupling)	312.97	396.2	314.65	398.5
VCWG_EP (two-way coupling)	314.65	423.85	317.35	428.29
VCWG_EP_Profile (two-way coupling)	356.73	503.39	364.43	522.3

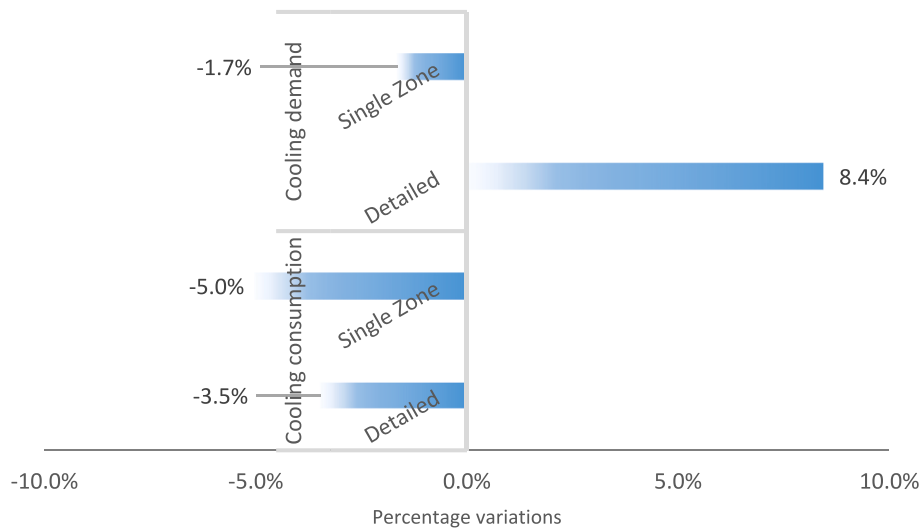


Fig. 11. Variations of cooling consumption and demand for medium office buildings between two-way coupling and one-way coupling (positive “+” sign indicates increases in cooling consumption or demand, negative “-” sign indicates decreases in cooling consumption or demand).

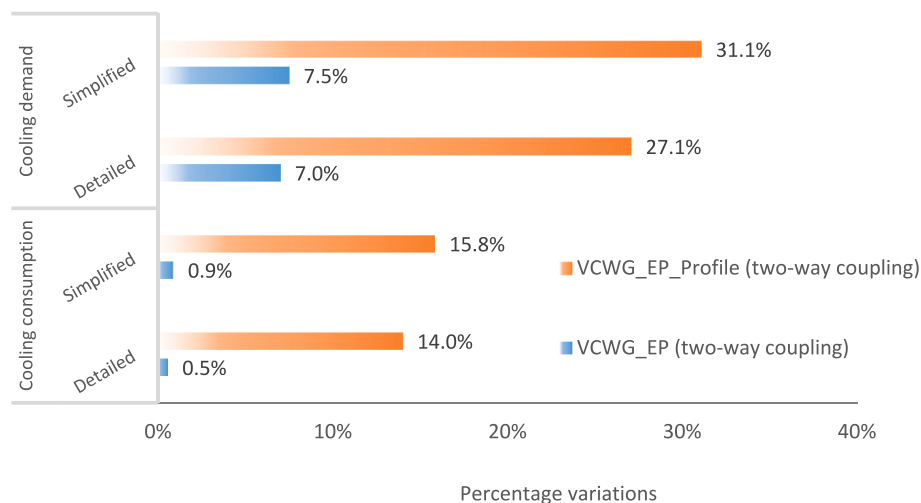


Fig. 12. Variations of cooling consumption and demand for high-rise office buildings between two-way coupling and one-way coupling (positive “+” sign indicates increases in cooling consumption or demand, negative “-” sign indicates decreases in cooling consumption or demand).

cooling consumption with the two-way coupling approaches (VCWG_EP two-way and VCWG_EP_Profile two-way) in comparison with those with one-way coupling method for the high-rise office building model. Cooling energy consumption and cooling demands using the VCWG_EP two-way coupling are increased by 0.5 % and 7.0 %, respectively in comparison with the prediction results using VCWG_EP one-way coupling approach for the detailed high-rise office building model. For the simplified building model, we observe comparable percents of

increase in cooling energy consumption (0.9 %) and cooling demands (7.5 %) to those for the detailed high-rise office building model when using the VCWG_EP two-way coupling approach.

Adopting the VCWG_EP_Profile two-way coupling approach results in substantial increases in both cooling energy and demands for the high-rise office building model. As shown in Fig. 12, for the detailed high-rise office building model, cooling energy consumption and cooling demand using the VCWG_EP_Profile two-way coupling approach are

increased by 14.0 % and 27.1 %, respectively in comparison with the prediction results using VCWG_EP one-way coupling approach. The complex two-way coupling approach with environmental data exchange at various building levels is thus recommended for modeling tall buildings at an urban scale. The computation times for VCWG_EP two-way and VCWG_EP_Profile two-way are close. Enhanced modeling performance for tall buildings comes from the combined effects of dynamic coupling, feeding the building energy waste heat flux back into the urban physics model, and detailed local climate profiles varying with height. The impact of model complexity on computational time is relatively small based on the tested cases coupling EnergyPlus and VCWG for a single building (either medium office building or high-rise office building). The computational time is the sum of the simulation time of the two programs (EnergyPlus and VCWG) and the time required for data exchange between the two programs. The current computational times for two-way coupling scenarios are about one order of magnitude greater than the time required for EnergyPlus simulations alone. The computational time would vary with the computing hardware and actual code implementation. Deviations in computational times due to model complexity and coupling approaches may be expected for urban-scale building energy modeling.

6. Conclusion

The thermal performance of individual buildings is influenced by their surrounding built and climatic environment. However, the lack of an urban building energy modeling framework that considers the influence of the surrounding built and climatic environment on building thermal performance leads to inaccurate urban scale modeling results. This study investigates dynamic coupling methods between the urban physics model VCWG and the whole building energy program EnergyPlus. Particularly, VCWG provides to EnergyPlus the predicted local conditions of the urban microclimate such as canyon temperature, relative humidity and roof convective heat transfer coefficient; EnergyPlus predicts building heat dissipations and building exterior surface temperatures and passes both waste heat generated by HVAC systems and surface temperatures to VCWG.

These coupling approaches include embedding a single zone energy model in an urban physics model (VCWG); running the urban physics model first to generate an urban weather file followed by running building energy models (VCWG_EP, one-way coupling); and interactive coupling between VCWG and EnergyPlus during each time step (VCWG_EP, two-way coupling). In VCWG_EP (one-way coupling), VCWG was run first to generate a local weather file representing urban microclimate conditions and then the EnergyPlus model was simulated using the local weather file. A more complex coupling approach (VCWG_EP_Profile, two-way coupling) was evaluated for the high-rise office building case. In VCWG_EP_Profile (two-way coupling), detailed profiles varying with heights for wall surface temperatures and HVAC heat dissipations were passed from EnergyPlus to VCWG at each time step and similarly, detailed profiles of canyon temperature and relative humidity varying with height besides roof convective heat transfer coefficient were fed to EnergyPlus from VCWG. The impacts of coupling approaches and model complexity on canyon temperature and building energy profiles are evaluated using two case studies.

We tested and validated the coupling method using three field measurements: BUBBLE in Basel, Switzerland, the CAPITOU experiment in Toulouse, France, and the Sunset neighborhood field measurement in Vancouver, Canada. Sensitivity analyses evaluated the impacts of urban geometric and surface features on canyon temperature, building energy consumption, and demand. With the combination of roof to canyon width ratio (0.75, 1, 1.5, 3), canyon orientation (-45° , 90°), and ground vegetation fraction (0, 0.5, 1), cooling electricity consumption varies between -6.6% and 14.9% and the cooling demand variation ranges from -8.8% to 17.5% using the coupled VCWG_EP simulations for the medium office building located in Chicago, IL in comparison with

the baseline scenario (roof to canyon width ratio = 1, canyon orientation = 90° , and ground vegetation fraction = 0).

We used two synthetic building models to demonstrate the impacts of building energy model complexity (simplified/single zone vs. detailed/multi-zone models) and different coupling approaches on canyon temperature and building energy profiles. We illustrate the qualitative impacts of model complexity and coupling on canyon temperature and energy use/demands using Fig. 13 (color-coded) for the high-rise office building model. We categorize the impacts into minimum, medium, and significant.

Fig. 13 helps us visualize two key findings from our study. First, the level of EnergyPlus model complexity has limited impacts on urban canyon temperature based on the similar color pattern indicating qualitative impacts between detailed and simplified building energy models. In fact, the differences in canyon average, maximum, and minimum temperatures are within 0.3°C . The differences in cooling energy consumption and demands between detailed and simplified single-zone models are mainly from the deviations of EnergyPlus baseline models. Second, significant differences in maximum canyon temperature and cooling energy profiles between the VCWG_EP_Profile two-way coupling approach and VCWG_EP two-way coupling as well as one-way coupling approaches suggest that adopting a complex two-way coupling approach with environmental data exchange at various building levels is necessary for modeling tall buildings at an urban scale.

We compared and analyzed VCWG_EP one-way coupling, VCWG_EP two-way coupling, and VCWG_EP_Profile two-way coupling in this study. Specific findings for the medium office building and the high-rise office building are summarized below.

- The differences in average, maximum, and minimum canyon temperature between VCWG_EP one-way coupling and VCWG_EP two-way coupling are up to 0.46°C for the medium office building and up to 1.55°C for the high-rise office building.
- Utilizing VCWG_EP_Profile two-way coupling has a significant effect on canyon temperature for the high-rise building model, resulting in an increase of up to 1.38°C in average temperature and an increase of up to 5.80°C in maximum temperature in comparison with VCWG_EP (one-way coupling).
- Cooling energy consumption and cooling demands using the VCWG_EP two-way coupling approach decreased by 3.5 % and increased by 8.4 %, respectively in comparison with the prediction results using VCWG_EP one-way coupling approach for the detailed medium office building model.
- Cooling energy consumption and cooling demands using the VCWG_EP two-way coupling approach increased by 0.5 % and 7.0 %, respectively in comparison with the prediction results using VCWG_EP one-way coupling approach for the detailed high-rise office building model.
- Cooling energy consumption and cooling demands using the VCWG_EP_Profile two-way coupling approach increased by 14.0 % and 27.1 %, respectively in comparison with the prediction results using VCWG_EP one-way coupling approach for the detailed high-rise office building model.

This study on interactive coupled modeling engages urban physics models such as VCWG and UWG, which use periodic features for urban geometry and ground surface conditions to represent urban canyons. The inclusion of regional weather or climate models may help better describe realistic neighborhood settings. The proposed dynamic coupling method between the urban physics model VCWG and the whole building energy program EnergyPlus can be extended to large-scale building energy modeling for sustainable and resilient future communities and cities.

High-Rise Office Building	Detailed Model		Simplified Model	
	VCWG_EP	VCWG_EP_Profile	VCWG_EP	VCWG_EP_Profile
Canyon Temperature (Average)	Minimum	Medium	Minimum	Medium
Canyon Temperature (Maximum)	Medium	Significant	Medium	Significant
Canyon Temperature (Minimum)	Minimum	Medium	Minimum	Medium
Cooling Energy Consumption	Minimum	Significant	Minimum	Significant
Cooling Demands	Medium	Significant	Medium	Significant

Minimum
Medium
Significant

Fig. 13. Summary matrix for the impacts of model complexity and coupling on canyon temperature and energy use/demands.

CRedit authorship contribution statement

Liping Wang: Writing – review & editing, Writing – original draft, Validation, Methodology, Funding acquisition, Formal analysis, Conceptualization. **Lichen Wu:** Writing – review & editing, Validation, Software, Methodology, Formal analysis, Data curation. **Leslie Keith Norford:** Writing – review & editing, Validation, Methodology, Formal analysis, Conceptualization. **Amir A. Aliabadi:** Writing – review & editing, Validation, Methodology, Formal analysis, Conceptualization. **Edwin Lee:** Writing – review & editing, Software, Methodology.

Declaration of competing interest

The authors declare that they have no known competing financial interests or personal relationships that could have appeared to influence the work reported in this paper.

Data availability

Data will be made available on request.

Acknowledgment

This study is supported by the National Science Foundation Environmental Sustainability program under Grant No. CBET 1944823. Any opinions, findings, conclusions, or recommendations expressed in this material are those of the authors and do not necessarily reflect the views of the National Science Foundation.

References

- [1] The United States Department of State and the United States Executive Office of the President, *The Long-Term Strategy of the United States: Pathways to Net-Zero Greenhouse Gas Emissions by 2050*, 2021.
- [2] United Nations environment programme, *Cities and climate change*. <https://www.unep.org/explore-topics/resource-efficiency/what-we-do/cities/cities-and-climate-change>.
- [3] United Nations, *68% of the world population projected to live in urban areas by 2050, 2018*. <https://www.un.org/development/desa/en/news/population/2018-revision-of-world-urbanization-prospects.html>.
- [4] IPCC, *Summary for Policymakers—Climate Change 2021: the Physical Science Basis*, 2021.
- [5] IPCC, *Global Warming of 1.5°C: IPCC Special Report on Impacts of Global Warming of 1.5°C above Pre-industrial Levels in Context of Strengthening Response to Climate Change, Sustainable Development, and Efforts to Eradicate Poverty*, Cambridge University Press, Cambridge, 2022.
- [6] D.J. Sailor, A review of methods for estimating anthropogenic heat and moisture emissions in the urban environment, *Int. J. Climatol.* 31 (2) (2011) 189–199.
- [7] E. Erell, T. Williamson, Intra-urban differences in canopy layer air temperature at a mid-latitude city. *International Journal of Climatology* 27 (9) (2007) 1243–1255.
- [8] B. Bueno, et al., Computationally efficient prediction of canopy level urban air temperature at the neighbourhood scale, *Urban Clim.* 9 (2014) 35–53.
- [9] M. Santamouris, Recent progress on urban overheating and heat island research. Integrated assessment of the energy, environmental, vulnerability and health impact, *Synergies Global Clim. Change. Energy Build.* 207 (2020), 109482.
- [10] C.F. Reinhart, C. Cerezo Davila, Urban building energy modeling – a review of a nascent field, *Build. Environ.* 97 (2016) 196–202.
- [11] B. Bueno, et al., Combining a detailed building energy model with a physically-based urban canopy model, *Boundary-Layer Meteorol.* 140 (3) (2011) 471–489.
- [12] C. Reinhart, et al., Umi-an urban simulation environment for building energy use, daylighting and walkability, in: *13th Conference of International Building Performance Simulation Association*, Chambéry, France, 2013.
- [13] N.H. Wong, et al., An integrated multiscale urban microclimate model for the urban thermal environment, *Urban Clim.* 35 (2021), 100730.
- [14] F. Salamanca, et al., A new building energy model coupled with an urban canopy parameterization for urban climate simulations—part I. formulation, verification, and sensitivity analysis of the model, *Theor. Appl. Climatol.* 99 (3) (2009) 331.
- [15] L.A. Bollinger, R. Evins, Hues: A Holistic Urban Energy Simulation Platform For Effective Model Integration, in: *Proceedings of International Conference CISBAT 2015 Future Buildings and Districts Sustainability from Nano to Urban Scale*, 2015.
- [16] L. Swan, V. Ugursal, I. Beausoleil-Morrison, Implementation of a Canadian residential energy end-use model for assessing new technology impacts, in: *IBPSA 2009-International Building Performance Simulation Association 2009*, 2009.
- [17] B. Bueno, et al., Development and evaluation of a building energy model integrated in the TEB scheme. *Geosci. Model Dev.* 5 (2) (2012) 433–448.
- [18] R. Baetens, et al., Assessing electrical bottlenecks at feeder level for residential net zero-energy buildings by integrated system simulation, *Appl. Energy* 96 (2012) 74–83.
- [19] B. Bueno, et al., A resistance-capacitance network model for the analysis of the interactions between the energy performance of buildings and the urban climate, *Build. Environ.* 54 (2012) 116–125.
- [20] D. Robinson, et al., *CITYSIM: Comprehensive Micro-simulation of Resource Flows for Sustainable Urban Planning*, 2009.
- [21] P. Remmen, et al., CityGML import and export for dynamic building performance simulation in modelica, *Build. Performance Model. Conf.* (2016).
- [22] R. Nouvel, et al., SimStadt, a New Workflow-Driven Urban Energy Simulation Platform for CityGML City Models. *CISBAT 2015, EPFL, Lausanne*, 2015. September 9–11th.
- [23] A. Rahman, V. Srikumar, A.D. Smith, Predicting electricity consumption for commercial and residential buildings using deep recurrent neural networks, *Appl. Energy* 212 (2018) 372–385.
- [24] Y. Chen, T. Hong, M. Piette, City-scale building retrofit analysis: a case study using CityBES, *Build. Simulat.* (2017).
- [25] R.E. Best, F. Flager, M.D. Lepech, Modeling and optimization of building mix and energy supply technology for urban districts, *Appl. Energy* 159 (2015) 161–177.
- [26] C. Molitor, et al., MESCOS—a multienergy system cosimulator for city district energy systems 10 (4) (2014) 2247–2256.
- [27] R. El Kontar, et al., *URBANopt: an Open-Source Software Development Kit for Community and Urban District Energy Modeling*, 2020.
- [28] É. Mata, A. Sasic Kalagasidis, F. Johnsson, Building-stock aggregation through archetype buildings: France, Germany, Spain and the UK, *Build. Environ.* 81 (2014) 270–282.
- [29] R.-L. Hwang, C.-Y. Lin, K.-T. Huang, Spatial and temporal analysis of urban heat island and global warming on residential thermal comfort and cooling energy in Taiwan, *Energy Build.* 152 (2017) 804–812.
- [30] T. Hong, et al., Urban microclimate and its impact on building performance: a case study of San Francisco, *Urban Clim.* 38 (2021), 100871.
- [31] J. Done, C.A. Davis, M. Weisman, The next generation of NWP: explicit forecasts of convection using the Weather Research and Forecasting (WRF) model, *Atmos. Sci. Lett.* 5 (6) (2004) 110–117.
- [32] B. Bueno, et al., The urban weather generator, *J. Build. Performance Simulat.* 6 (4) (2013) 269–281.
- [33] M. Moradi, E.S. Krayenhoff, A.A. Aliabadi, A comprehensive indoor–outdoor urban climate model with hydrology: the Vertical City Weather Generator (VCWG v2.0.0), *Build. Environ.* 207 (2022), 108406.
- [34] M. Moradi, et al., The vertical city weather generator (VCWG v1.3.2), *Geosci. Model Dev. (GMD)* 14 (2) (2021) 961–984.
- [35] A. Martilli, A. Clappier, M.W. Rotach, An urban surface exchange parameterisation for mesoscale models, *Boundary-Layer Meteorol.* 104 (2) (2002) 261–304.
- [36] J.C. Teixeira, et al., Surface to boundary layer coupling in the urban area of Lisbon comparing different urban canopy models in WRF, *Urban Clim.* 28 (2019), 100454.
- [37] K. Gohil, M.S. Jin, Validation and improvement of the WRF building environment parametrization (BEP) urban scheme, *Climate* 7 (9) (2019) 109.

- [38] D. Li, E. Bou-Zeid, Quality and sensitivity of high-resolution numerical simulation of urban heat islands, *Environ. Res. Lett.* 9 (5) (2014), 055001.
- [39] I. Ribeiro, et al., Highly resolved WRF-BEP/BEM simulations over Barcelona urban area with LCZ, *Atmos. Res.* 248 (2021), 105220.
- [40] M. Martin, et al., Comparison between simplified and detailed EnergyPlus models coupled with an urban canopy model, *Energy Build.* 157 (2017) 116–125.
- [41] M.W. Rotach, et al., Bubble – an urban boundary layer meteorology project, *Theor. Appl. Climatol.* 81 (3) (2005) 231–261.
- [42] V. Masson, et al., The canopy and aerosol particles interactions in Toulouse urban layer (CAPITOL) experiment, *Meteorol. Atmos. Phys.* 102 (3) (2008) 135.
- [43] B. Crawford, A. Christen, Spatial source attribution of measured urban eddy covariance CO₂ fluxes, *Theor. Appl. Climatol.* 119 (3) (2015) 733–755.
- [44] DOE, EnergyPlus Energy Simulation Software, Version 22.1.0, 2022. Available from: <https://github.com/NREL/EnergyPlus/releases/tag/v22.1.0>.
- [45] ASHRAE, ASHRAE Guideline 14: Measurement of Energy, Demand and Water Savings, American Society of Heating, Refrigeration and Air Conditioning Engineers, Atlanta, GA, 2014.